Accepted Manuscript

Pumping Test Analysis Using a Layered Cylindrical Grid Numerical Model in a Complex, Heterogeneous Chalk Aquifer

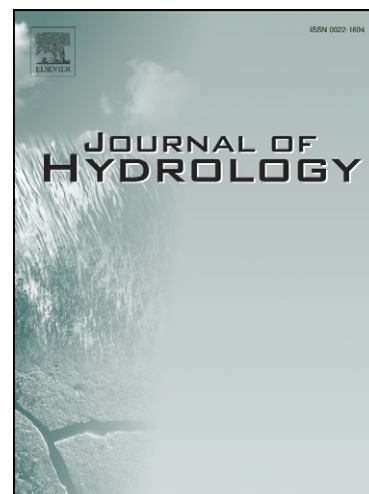M.M. Mansour, A.G. Hughes, A.E.F. Spink, J. Riches

Please cite this article as: Mansour, M.M., Hughes, A.G., Spink, A.E.F., Riches, J., Pumping Test Analysis Using a Layered Cylindrical Grid Numerical Model in a Complex, Heterogeneous Chalk Aquifer, *Journal of Hydrology* (2011), doi: 10.1016/j.jhydrol.2011.02.005

1   Title page:

2   **Pumping Test Analysis Using a Layered Cylindrical Grid Numerical**

3   **Model in a Complex, Heterogeneous Chalk Aquifer.**

4   M. M. Mansour, A. G. Hughes, A. E. F. Spink, J. Riches

5   **First author**
6   First name: Majdi
7   Middle Name: M
8   Last Name: Mansour
9   Academic degrees: BSc, MSc, PhD.
10   Affiliation: Senior Scientific Officer. British Geological Survey. Keyworth.
11   Nottingham. UK
12   Email: majm@bgs.ac.uk
13   Address: British Geological Survey
14   Kingsley Dunham Centre
15   Keyworth,
16   Nottingham, UK
17   NG12 5GG
18
19   **Contributing author 1**
20   First name: Andrew
21   Middle Name: G
22   Last Name: Hughes
23   Academic degrees: BSc, MSc, PhD.
24   Affiliation: Principal Scientist Officer. British Geological Survey. Keyworth.
25   Nottingham. UK
26   Email: aghug@bgs.ac.uk
27
28
29   **Contributing author 2**
30   First name: Andrew
31   Middle Name: E.F.
32   Last Name: Spink
33   Academic degrees: BSc, MSc, PhD.
34   Affiliation: Lecturer in Groundwater. The University of Birmingham.
35   Birmingham. UK
36   Email: a.e.f.spink@bham.ac.uk
37
38   **Contributing author 3**
39   First name: Jamie
40   Middle Name:
41   Last Name: Riches
42   Academic degrees: BSc, MSc.
43   Affiliation: Groundwater Resources Consultant. Thames Water. Reading. UK
44   Email: Jamie.Riches@thameswater.co.uk
45
46

1

47 **Pumping Test Analysis Using a Layered Cylindrical Grid Numerical**

48 **Model in a Complex, Heterogeneous Chalk Aquifer.**

49 M. M. Mansour, A. G. Hughes, A. E. F. Spink, J. Riches

50 **Abstract**

51 A groundwater investigation including several pumping tests has been carried out by

52 Thames Water Utilities Limited (TWUL) to improve the understanding of the

53 distribution of hydraulic properties of the Chalk in the Swanscombe area of Kent in

54 south-eastern England. The pumping test behaviour is complicated by: the fractured

55 condition of the Chalk, simultaneous pumping from adjacent boreholes, and variable

56 pumping rates during the test. In addition, the groundwater flow system is

57 complicated by quarrying of the Chalk. Analytical solutions for pumping test analysis

58 fail to represent these complex flow processes and cannot reproduce the observed

59 time drawdown curves. A layered cylindrical grid numerical model has been applied

60 to the results of the Swanscombe pumping test. This model can represent the

61 heterogeneity of the aquifer and the detailed flow processes close to the abstraction

62 borehole such as well storage, seepage face and well losses. It also includes a

63 numerical representation of the moving water table using a grid that deforms to

64 eliminate numerical instabilities. The analyses of the test results demonstrate that

65 they are significantly influenced by fracture flow, which needs to be included to

66 improve the simulation of the groundwater system; not withstanding this, the layered

67 cylindrical grid numerical model reproduced many of the features in observed time-

68 drawdown, which allowed an assessment of the hydraulic characteristics of the

69 aquifer as well as the investigation of the impact of quarries on the test results. This

70 has demonstrated that the numerical model is a powerful tool that can be used to

71   analyse complex pumping tests and aid to improvement of the conceptual

72   understanding of a groundwater system.

73   **1.0   Introduction**

74   During the later part of 2002, a multiple borehole pumping test was conducted by

75   Thames Water Utilities Limited (TWUL) to understand the hydraulic properties of the

76   Chalk aquifer, in the Swanscombe area of Kent in south-eastern England, and to

77   assess abstraction sustainability (Fig. 1). Pumping tests are controlled field

78   experiments carried out to determine the hydraulic properties of an aquifer or to

79   validate a conceptual model of a groundwater system (BSI 1992). Such tests yield

80   plots of time-drawdown values which exhibit a behaviour dictated by the hydraulic

81   characteristics of the aquifer. Under ideal conditions, this behaviour can be

82   represented by analytical solutions to obtain the values of the hydraulic parameters of

83   the aquifer. Typical time-drawdown plots, produced by these analytical solutions,

84   have been described by a number of researchers, for example Neuman (1971, 1979),

85   Streltsova (1972, 1973), Gambolati (1976), and Kruseman and de Ridder (1990).

86   Previous studies of Chalk aquifer properties show that the transmissivity and storage

87   coefficient vary spatially depending on the geological development of the Chalk

88   (Allen et al. 1997). The development of fractures complicates the groundwater flow

89   behaviour and solution processes greatly affect the characteristics of the Chalk and the

90   flow mechanisms within it, which is often referred to as dual-porosity. It is, therefore,

91   anticipated that the hydraulic properties of the Chalk in the Swanscombe area will be

92   spatially variable, causing the time-drawdown curves to deviate from the typical plots.

93   This deviation is potentially exacerbated by: the existence of large active sub-water

94   table quarries (Fig. 2a); simultaneous abstraction from adjacent boreholes leading to

95   interfering cones of depression; and because of the occurrence of generator outages

3

96   causing random interruption to abstraction and unplanned periods of groundwater

97   head recovery. Consequently, the commonly used analytical solutions such as

98   Theis (1935) solution and the Cooper and Jacob (1946) approximation for analysing

99   pumping tests in confined aquifers, the Hantush-Jacob (1955) solution for leaky

100   aquifers, Boulton's (1954) model, Dagan's (1967) solution and Neuman's (1972)

101   equations for tests in unconfined aquifers cannot be applied effectively to the

102   Swanscombe pumping test. Other analytical solutions such as the analytical solution

103   for partially penetrating wells in unconfined aquifers (Neuman 1974) or (Moench

104   1993; 1994), the analytical solution that accounts for pumping from large diameter

105   wells in unconfined aquifers (Moench 1997), the solution for unsteady flows in

106   single-porosity or double-porosity confined aquifers (Barker 1988), etc. target specific

107   problems and cannot simulate the flow processes of this complex pumping test. A

108   numerical layered cylindrical grid model is applied to improve the conceptual

109   understanding of the system, especially the impact of quarries and to determine the

110   values of the hydraulic parameters of the Chalk aquifer. This paper demonstrates that

111   this numerical model is a flexible tool that can be applied to answer questions

112   imposed by the conceptual model, in this case the effect of quarries, and improves it.

113   It also demonstrates that despite the complexity of the Chalk groundwater system, the

114   numerical model can reproduce satisfactorily much of the behaviour of the observed

115   time-drawdown curves, allowing a better understanding of the aquifer hydraulic

116   characteristics.

117

118   **2.0   Materials and methods**

119   The Swanscombe area is located on the south-eastern side of the London Basin

120   (Fig 1). It comprises the main valley of the River Thames, bordered by wide terraces,

121   and Palaeogene age deposits over a Chalk plateau, which is terminated by an

4

122   escarpment to the south. The Chalk has a maximum thickness of approximately

123   200 m and is partly covered by Palaeogene deposits comprising the Lambeth Group

124   and the Thames Group. Along the Thames in the north of the area, the Chalk is

125   overlain by terrace deposits and riverine alluvium. The regional hydraulic gradient

126   slopes from the North Downs escarpment northwards towards the Thames. The area

127   is drained by the River Thames to the north, the Rivers Cray and Darent in the west

128   and the Rivers Ebbsfleet and Medway in the east. For further information about the

129   regional hydraulic gradient refer to Darling et al (2010).

130   Characteristic of the Swanscombe area is an abundance of raw materials that are

131   utilised by the cement industry: chalk, clay and alluvial deposits are worked and

132   gravel extraction is also common. Several sub-water-table quarries have been

133   abandoned as the costs of dewatering have exceeded the rewards from quarrying.

134   Other quarries are reaching their maximum development depth and, when they close,

135   pumping will cease. Two quarries in particular form the focus of this study; the

136   Eastern Quarry, which is ceased operating in late 2007 and the Western Quarry, which

137   has now been developed into a shopping centre.

138   The pumping test involved two abstraction wells plus four abstraction boreholes and

139   thirty-one observation boreholes (Fig. 2). The two abstraction wells, defined as such

140   on the basis of their large diameter size, are the Greenhithe abstraction well and the

141   Southfleet abstraction well. Greenhithe abstraction well is located near the north-

142   western corner of Eastern Quarry approximately 150 m from its western edge, and

143   Southfleet abstraction well is close to the Eastern Quarry and located approximately

144   550 m from its eastern side (Fig. 2a). These two pumping wells are approximately

145   2700 m apart. The four abstraction boreholes, defined as such on the basis of their

146   relatively small diameter size, are located in the area south of the quarries. These

147   boreholes are: Site A (the Western Bean Farm borehole), Site B (the West Drudgeon

148   Farm borehole), Site C (the Mid Drudgeon Farm borehole) and Site D (the West

149   Beacon Wood borehole). Of the four abstraction boreholes, Site A is closest to the

150   Greenhithe well at a distance of 1800 m and Site C is the closest to Southfleet at a

151   distance of 2000 m. A distance of approximately 1300 m separates Sites A and C.

152   Pumping started on 18 October 2002 at sites A, B, and C with abstraction rates of

153   19.0 l/s, 12.7 l/s and 77.5 l/s respectively. Abstraction at Site D started eight days

154   later at a rate of 49.0 l/s. Abstraction at Greenhithe and Southfleet started 28 days

155   later at rates of 46.0 l/s and 37.0 l/s respectively. The abstraction at all sites ceased on

156   the 16 December 2002 and the recovery at the abstraction boreholes was recorded for

157   a further two days. During the pumping phase, abstraction was interrupted randomly

158   at all the sites either because of generator failures or for generator maintenance,

159   leading to unplanned recovery periods. This paper focuses on the results obtained at

160   Site C and two of its neighbouring observation boreholes, boreholes 12 and 19, to

161   illustrate the complexity of the Chalk groundwater system and the advantages of using

162   the numerical radial flow model to simulate this groundwater system and analyse the

163   pumping test results. The observed drawdown results are shown in Figures 5 and 6.

164   **3.0   Theory/calculation**

165   The layered cylindrical grid numerical model uses the finite-difference method to

166   solve the basic equation describing flow through a porous medium under confined and

167   unconfined conditions. To simulate groundwater flow converging to a pumped well,

168   the three-dimensional basic flow equation is written in cylindrical coordinates and the

169   aquifer is discretised using a grid illustrated in Figure 3. For confined aquifers and in

170   terms of the drawdown (*s*) this equation is given by (Rushton 2003):

171    $$K_r \frac{\partial^2 s}{\partial r^2} + \frac{K_r}{r} \frac{\partial s}{\partial r} + \frac{K_\theta}{r^2} \frac{\partial^2 s}{\partial \theta^2} + \frac{K_z}{r^2} \frac{\partial^2 s}{\partial z^2} = S_s \frac{\partial s}{\partial t} + N \qquad \text{Equation 1}$$

6

172   Where:

173   K_r, K_θ and K_z are the hydraulic conductivities in the radial, the

174   circumferential and the vertical directions respectively.   (LT^{-1})

175   S_s is the specific storage   (L^{-1})

176   N is an external source term.   (T^{-1})

177   r is the radius from the centre of the abstraction borehole to the point where

178   the drawdown s is calculated   (L)

179 In a layered system, the head values of Equation 1 are averaged over the layer

180 saturated thickness and the horizontal hydraulic conductivity is replaced by the

181 transmissivity of the layer. This does not apply at the uppermost layer if the

182 groundwater system is under unconfined conditions. Under these conditions an

183 additional numerical layer is created at the top of the uppermost layer of the model to

184 represent the presence of the water table (Fig. 3).

185 The equation that describes the movement of the water table is discussed by Todsen

186 (1971) and Neuman (1972) and is given by:

187 $$\frac{\partial \varphi}{\partial t} = \frac{-1}{n_e}\left(K_r \frac{\partial s}{\partial r}\frac{\partial \varphi}{\partial r} + \frac{K_\theta}{r^2}\frac{\partial s}{\partial \theta}\frac{\partial \varphi}{\partial \theta} - K_z \frac{\partial s}{\partial z}\right)$$ Equation 2

188 Where:

189   φ is a function that represents the location of the water table and   (L)

190   n_e is the porosity of the aquifer.   (Dimensionless)

191 The complexity of this non-linear equation can be reduced by assuming that the

192 product of the hydraulic gradients is small and can be neglected (Rushton and

193 Redshaw 1979). In this case Equation 2 reduces to: $\frac{\partial \varphi}{\partial t} = \frac{1}{S_y}\left(K_z \frac{\partial s}{\partial z}\right)$ where the

194 porosity is considered to be approximately equal to the specific yield S_y. By changing

195 the subject, this equation can be written as: $K_z \dfrac{\partial s}{\partial z} = S_y \dfrac{\partial \varphi}{\partial t}$ and then by Darcy's law:

196 $q_z = S_y \dfrac{\partial \varphi}{\partial t}$, allowing the term q_z to be added to the right hand side of Equation 1,

197 which is then applied only to the water table nodes. The radial interval between nodes

198 increases in a logarithmic pattern from the centre of the abstraction borehole where

199 the numerical grid is centred to the outer boundary. This creates a large number of

200 nodes close to the abstraction well and improves the representation of the steep

201 hydraulic gradient as a result of pumping in the vicinity of the abstraction borehole.

202 In contrast to a general saturated aquifer node, a water table node changes its location

203 vertically based on its head value calculated at the end of a time step (Fig. 3). This

204 allows the aquifer to dewater as the water table moves downwards and the saturated

205 thickness of the uppermost layer becomes spatially variable.   The vertical flow

206 between nodes in different layers is determined by considering mass conservation at

207 the interface between layers.

208 To represent the water contained within the abstraction well, i.e. well storage, the

209 values storage coefficients of the nodes located inside the abstraction borehole and

210 where pumping is applied are all set to unity. The occurrence of the seepage face is

211 represented by acknowledging that the aquifer nodes located at the abstraction

212 borehole face became subject to atmospheric pressure when the water levels inside the

213 abstraction borehole drops below the base of their corresponding layers. When this

214 happens the groundwater head values of these nodes are fixed to a value equal to the

215 base elevations of their corresponding layers.

216 The model code has been developed in C++ programming language and benefits from

217 the object-oriented technology. Information on the application of this technology in

218 groundwater modelling can be found in the work of Spink et al. (2003) and

8

219   Jackson et al. (2003). For a full description of the model and its application refer to

220   Mansour (2003) and Mansour et al. (2003). This type of model is preferred to the

221   Cartesian grid groundwater models that allow grid refinement such as ZOOMQ3D

222   (Jackson et al. 2003) and MODFLOW 2005 (Harbaugh 2005) because of its better

223   representation of the flow processes taking place next to the abstraction borehole, e.g.

224   well losses, well storage, seepage face, etc. In addition, although the Cartesian grid

225   models yield accurate solutions at the observation boreholes, the solution at the

226   abstraction borehole is less accurate. The inaccuracy at the abstraction borehole is

227   primarily due to the structure of the Cartesian numerical grid, which does not allow

228   the specification of nodes at the well face and consequently it is not possible to set the

229   hydraulic conductance values between the node inside the well and its surrounding

230   aquifer nodes correctly. In addition, it is not possible to set both the area and the

231   perimeter of a rectangular cell in a Cartesian model to be equal to the area and

232   perimeter of the actual circular abstraction borehole at the same time. If the numerical

233   grid is refined so that the area of the rectangular cell is equal to the area of the

234   abstraction borehole the rectangular cell will have a perimeter that is smaller than the

235   actual borehole perimeter. As the area through which groundwater is flowing from

236   the aquifer to the abstraction borehole in the numerical model is smaller than in

237   reality, it causes the simulated drawdown to be greater than the observed one.

238   The preprocessor, RADMOD (Reilly and Harbaugh 1993), has been developed for

239   MODFLOW (McDonald and Harbaugh 1988) to simulate axi-symmetric flow to a

240   well. The radial flow model reported here has the advantage of simulating the moving

241   water table, which cannot be done in RADMOD.

242

9

4.0   Results and discussion

4.1   Conceptual model

The Chalk aquifer is partly overlain by Palaeogene strata in the Swanscombe area

(Fig. 1 and Fig. 2). However, the water table is within the Chalk Formation almost

everywhere and the Chalk is the only source of groundwater available for abstraction.

While groundwater flow in the Chalk is complicated by the presence of fractures or

high conductivity zones as demonstrated in the analysis of an earlier individual

pumping test (Spink and Mansour 2003), it has not been possible to determine the

size, extents, and directions of these high conductivity zones. Consequently, these

zones cannot be represented in details in the conceptual model and the Chalk aquifer

is represented here using two uniform hydro-geological layers. The upper one, in

which the high conductivity zones are better developed, is in direct contact with the

abstraction borehole at Site C. The lower layer, which represents the remainder of the

Chalk and is less well developed, is also included as it may contribute to the total

water abstracted (Fig. 2b). Aquifer permeability values obtained from the analysis of

the pumping test are related, therefore, to both the Chalk matrix and the fractures or

high conductivity zones within it.

The layered cylindrical grid model can address conceptual complexities related to the

representation of flow processes next to the abstraction borehole, the variation of

pumping rates, and the simultaneous pumping from more than one borehole.

However, the effects of the quarries on the pumping test results are not fully

understood. The quarries may cause an increase in drawdown because of the reduced

aquifer thickness in the zone where the aquifer is missing and through which

groundwater flows are converging towards the abstraction well. Conversely, it may

be also possible that the water held in the topographical depressions on the surface of

10

268   these quarries provides the system with a source of water which compensates the

269   effects of the missing part of the aquifer. These two conceptual representations of the

270   quarries are investigated by the numerical model.

271

272   *4.2   Overview of the test results: preliminary assessment*

273   The time-drawdown curve of the first abstraction phase at Site C (Fig. 5 Phase 1) does

274   not show the typical unconfined behaviour because of the step increases in the

275   pumping rate at the start of the test. The typical behaviour of a time-drawdown curve

276   in unconfined aquifers, as explained by Kruseman and de Ridder (1990), has an 'S'

277   shape (Fig. 4a) when plotted on logarithmic axes. Each section of the S curve reflects

278   the changes in the dominant process occurring in the aquifer. At early times, the

279   abstracted water is released instantaneously from storage by the expansion of the

280   water and the compaction of the aquifer. The unconfined aquifer effectively behaves

281   as confined, but the time-drawdown curve may not match the Theis solution because

282   of well storage, which delays the start of drawdown at the observation boreholes

283   (Zone 1 of Fig. 4a). Once the water table starts falling, the quantity of water released

284   from specific yield (S_y) reduces the gradient of the intermediate-time segment and the

285   time-drawdown curve is comparable to that obtained from a leaky aquifer (Zone 2 of

286   Fig. 4a). In the third stage, the time-drawdown curve once again tends to conform to

287   a Theis curve based on storage due to S_y. At this time, the water table is the major

288   contributor to the water abstracted from the aquifer (Zone 3 of Fig. 4a).

289   When plotted on logarithmic time and linear drawdown axes, the time-drawdown

290   curve also takes a typical shape that can be divided into three segments. The first is a

291   straight line that matches the Theis solution, if well storage is small (last part of the

292   curve in Zone 1 of Fig. 4b). The second starts when the straight line changes gradient

11

293   and flattens indicating that storage from water table is contributing to the system. The

294   length of the second segment depends on the vertical hydraulic conductivity and the

295   specific yield of the aquifer (Zone 2 of Fig. 4b). The third segment starts when the

296   rate of drawdown increases again reflecting the fall of the water table (Zone 3 of

297   Fig. 4b).

298   The plot of the first abstraction phase at Site C (Fig. 5 Phase 1) also shows a delayed

299   increase in the drawdown values at the start of the test indicating the presence of a

300   significant source of water which is likely to be well storage. The time-drawdown

301   curves of the subsequent abstraction phases, however, show typical unconfined

302   behaviour but do not reflect the expected water table movement at later times. The

303   presence of a larger well storage component is evident in these phases and is reflected

304   by the delayed fall at the start of each phase. The field data collected during the

305   recovery phase (Fig. 5 Phase 7) show a delayed initial rise that is probably due to

306   problems in the measuring device and cannot be used to confirm this large well

307   storage.

308

309   *4.3   Numerical analysis*

310   Site C abstraction borehole diameter is 0.42 m, with a depth of 137 m. It is cased to a

311   depth of 75 m below the ground surface. A 43 m layer of Palaeogene deposits

312   overlies the Chalk at this site but the initial water level is recorded at a depth of

313   77.1 m from the ground surface indicating that the water table is not found within the

314   Palaeogene strata. The pumping borehole is open along its full saturated depth.

315   While the casing of the Site C abstraction borehole has a diameter of 0.42 m,

316   geophysical well logging (Buckley 2003) indicates that this borehole is larger than its

317   nominal size in the open section. Accordingly, the well diameter used in the model is

12

318   increased to 0.6 m, which is the average diameter shown by the borehole logs. The

319   first part of the Chalk aquifer, which is in direct contact with the abstraction well, is

320   approximately 60 m thick at this position (Fig. 2b). It is represented numerically by

321   four layers, the three uppermost layers are 10 m thick and the lower one is 30 m thick.

322   The narrow thicknesses of the first three layers allow the formation of the seepage

323   face at the abstraction borehole wall. The second, deeper Chalk layer, which is not in

324   contact with the abstraction borehole (Fig. 2b), is approximately 108 m thick and

325   represented in the model by one numerical layer.

326   A three dimensional model was built to improve the representation of the quarries and

327   to improve the locations of the abstraction and observation boreholes within the

328   model. In a single slice numerical model, i.e. assuming radial symmetry and

329   simulating groundwater flow using the radial and vertical directions only, observation

330   borehole 12 coincides with Site D abstraction borehole and observation borehole 17

331   coincides with Site B abstraction borehole. Consequently, it is not possible to

332   simulate the groundwater heads at the observation wells correctly as they coincide

333   with the abstraction boreholes. The three-dimensional numerical model is built by

334   replicating the vertical cross section described above fourteen times along different

335   radial directions. The 14 slices provided a line of nodes along the radial direction

336   next to the abstraction and observation boreholes of interest (Fig. 2a). In three-

337   dimensional view the numerical model takes a form that is similar to the one shown in

338   Figure 3 but without the well casing. While the groundwater flow processes at

339   borehole Site C are represented in detail, the remaining pumping boreholes are

340   included in the model by assigning the corresponding abstraction to the nearest model

341   node (Fig. 2a).

13

342   The model was calibrated by modifying the values of the aquifer hydraulic parameters

343   until the simulated drawdown curves match the observed ones. Many trial values for

344   the aquifer parameters were used to match the simulated and field time drawdown

345   curves. Commencing with parameter values suggested by previous studies of the

346   Chalk (Allen et al. 1997), each trial involved changing the value of one parameter,

347   based on the effects that this parameter has on the relevant time-drawdown curves.

348   The parameters modified are: the horizontal and vertical hydraulic conductivities, the

349   specific yield and the specific storage of each layer of the model. Possible values for

350   the different hydraulic parameters can be established from this trial and error exercise.

351   To improve the fit between the numerical and field results the parameter estimation

352   package PEST (Doherty 2004) was used. PEST is model-independent software that

353   modifies the input files of the model and adjusts a preselected set of its parameters

354   until the discrepancy between the field and numerical results are reduced to a

355   minimum. PEST undertakes many model runs to optimise the parameter values and

356   to perform uncertainty analysis. PEST was used here to refine the hydraulic

357   parameter values and to estimate the uncertainty associated with these values.

358   Initially PEST was used without the inclusion of the quarries in the numerical model.

359   The parameters modified by PEST were: the horizontal and vertical hydraulic

360   conductivities, the specific yield and the specific storage, and the well loss factor.

361   The values of the hydraulic parameters optimised by PEST, as well as the estimated

362   95% confidence limits, are given in Table 1. The optimised transmissivity value of

363   the part of the Chalk that is in direct contact with the borehole is 1340 m^2 day^{-1}. The

364   optimised vertical hydraulic conductivity value is 0.86 m day^{-1}. The optimised

365   storage coefficient and specific yield are 1×10^{-5} m^{-1} and 0.012 respectively.

366   Subsequently, the quarries are added to the numerical model by altering the hydraulic

367   connections between the nodes to either remove the volume represented by the

368   quarries completely, or by reducing the thickness of the first layer of the Chalk, but

369   assuming that the water stored within the quarry is significant and is available to be

370   drawn by the abstraction boreholes.   Two additional runs were undertaken to

371   represent these conditions. In the first run the quarries were included in the model by

372   introducing internal impermeable boundaries along the quarry walls in the uppermost

373   numerical layer (numerical link (H) in Figure 3). The nodes located within the quarry

374   area, however, remained connected to the nodes underneath them by the mean of the

375   vertical hydraulic conductivity (numerical links (V) in Figure 3). Simulated

376   drawdown values produced from this run did not show significant differences from

377   the results when the quarry is ignored, because the internal boundaries do not greatly

378   affect the results and the vertical hydraulic connection was enough to withdraw water

379   from the specific yield storage of the nodes located within the quarry area. In the

380   second run the vertical connections between the nodes located within the quarries and

381   the nodes underneath them were both disconnected (Fig. 3). This run assumed that

382   the quarried Chalk was absent. The simulated drawdown values were influenced by

383   the disconnection of the nodes within the quarries, especially at the end of the

384   abstraction phases. These are the results presented in Figures 5 and 6.

385   Figure 5 shows a comparison between the simulated and observed drawdown values

386   at the abstraction borehole C. The numerical model reproduced satisfactorily the

387   steps in the time-drawdown curve of the first abstraction phase. In addition, the

388   simulated drawdown values and the gradient of the time-drawdown curve from

389   0.01days follow the observed ones, indicating that the hydraulic parameters used in

390   the numerical model are representative to the overall hydraulic characteristics of the

391   aquifer. The slight drawdown observed at approximately one day was produced after

392   the inclusion of quarries in the numerical model. The delayed decline recorded in the

393   field data (Fig. 5 Phase 2) suggests the presence of a larger well storage component

394   than is evident in the other phases. The field data collected during the recovery phase

395   (Fig. 5 Phase 7) show a delayed initial rise, but this may be due to a problem with the

396   measuring device. However, the numerical results do show an acceptable level of

397   recovery compared to the field data when abstraction is interrupted in the fourth

398   abstraction phase (Fig. 5 Phase 4).

399   Many of the observation boreholes show little response to pumping at the abstraction

400   boreholes and some of the observation boreholes show fluctuations in groundwater

401   levels that cannot be related to the pumping test. The only time-drawdown curves that

402   show reasonable correlation to abstraction at Site C are those at Bean Farm borehole

403   and Eastern Drudgeon Farm borehole, which are situated approximately 920 m and

404   240 m away from abstraction borehole C (Boreholes 12 and 19 in Fig. 2a). The match

405   between the simulated and drawdown values of the first two abstraction phases is

406   acceptable, indicating that the hydraulic conductivity and the storage coefficient

407   values, which control the gradient of the time-drawdown curve and the start of

408   drawdown respectively, are representative of the hydraulic characteristics of the

409   aquifer (Fig. 6). The behaviour of the simulated time-drawdown curves over the

410   remaining abstraction phases is comparable to the observed ones, but there are vertical

411   shifts between them. This is caused by the sudden drop in drawdown values at the

412   end of the second abstraction phase and is particularly evident in the Eastern

413   Drudgeon Farm borehole. This behaviour can be caused by the presence of fractures

414   that dry up when the water table falls beneath them leading to significant change in

415   the transmissivity of the Chalk aquifer. Fractured or high conductivity zones can be

416   modelled using the layered cylindrical grid model. However, in this instance it was

417   decided to concentrate on the impact of the quarries on the groundwater system.

418

419   **5.0   Conclusion**

420   This paper discusses the analysis of a complex pumping test undertaken in the Chalk

421   aquifer of the Swanscombe area, south-east London, using a numerical layered

422   cylindrical grid model.   The complexity of the Swanscombe pumping test arises from

423   factors such as abstraction from a partially penetrating abstraction borehole, the

424   stepwise increase of abstraction, the unplanned intermittent stoppages of pumping

425   during the test period and simultaneous pumping from adjacent boreholes. In

426   addition, the test results were affected by the presence of major quarries in the area.

427   Two scenarios are used to study the impact of the quarries on the test results. In the

428   first scenario, a quarry is represented in the model by imposing internal impermeable

429   boundaries along the locations of its walls whilst allowing the water stored within it to

430   contribute to the groundwater system. Quarries in this scenario did not impact the

431   simulated results. In the second scenario, in addition to the internal now flow

432   boundaries, the volume of water held by the quarries are completely removed from

433   the model. This quarry representation caused additional drawdown at the end of the

434   abstraction phases and improved the match between the observed and simulated time-

435   drawdown curves. This numerical configuration is used to estimate the hydraulic

436   parameter values of the aquifer.

437   The numerical results showed that a transmissivity value of 1340 m^2 day^{-1} of the part

438   of the Chalk that is in direct contact with the borehole, a vertical hydraulic

439   conductivity value of 0.86 m day^{-1}, and a storage coefficient and a specific yield of

440   1×10^{-5} m^{-1} and 0.012 respectively produce a good match between the observed and

17

441   simulated time drawdown curves. The use of the numerical model permitted the

442   deployment of the parameter estimation software PEST (Doherty 2004) to optimise

443   the values of the hydraulic parameters and to undertake uncertainty analysis. It was

444   found that the highest uncertainty was associated with the value of the storage

445   coefficient with the 95% confidence limits being approximately 45% greater or

446   smaller than the estimated value. The second highest uncertainty is associated with

447   the values of the specific yield and vertical hydraulic conductivity with the 95%

448   confidence limits being approximately 25% greater or smaller than the estimated

449   values (Table 1). These values fall within the limits reported in the literature for Chalk

450   aquifers (see for example Allen et al., 1997) and can be used to specify the hydraulic

451   parameter values for this site in a regional Cartesian model.

452   This paper demonstrates that the layered cylindrical grid model used in this study can

453   incorporate enough mechanisms to reproduce the complex behaviour of the time-

454   drawdown curve and has many advantages on the use of conventional analytical

455   solutions and on the Cartesian models which are not designed to simulate

456   groundwater flow converging to a pumped borehole. This work also demonstrates that

457   the cylindrical grid numerical model is a powerful tool for analysing the pumping test

458   results. It provides useful information on both the well performance and the hydraulic

459   characteristics of the aquifer which helps improving the conceptual model of aquifers

460   such as the complex Chalk aquifer.

461

462

463

464

465

466

467

468

469

470

471

472

473

474

475

476

477

478

479

480

481

482

483

484

485

486

487

488

489

490   **References**

491   Allen, D.J., Brewerton, L.J., Colbey, L.M., Gibbs, B.R., Lewis, M.A., Macdonald, A.M.,

492   Wagstaff, S.J., Williams, A.T,, 1997. The physical properties of major aquifers in England

493   and Wales. British Geological Survey Technical Report WD/97/34. Environment Agency R

494   & D Publication 8

495   Barker, J., 1988. A generalised radial-flow model for pumping tests in fractured rock. Water

496   Resources Research. 24, 10, 1796 – 1804.

497   Boulton, N.S., 1954. The drawdown of a water-table under non-steady conditions near a

498   pumped well in an unconfined formation. Proceedings of the Institution of Civil Engineers. 3,

499   Part 3, 564 – 579

500   BSI, 1992. Code of practice for Test pumping of water wells. BS 6316 : 1992. London, UK.

501   Buckley, D., 2003 Swanscombe Phase 2a Task 2.2 Geophysical Logging. British Geological

502   Survey Technical Report. CR/01/239C.

503   Cooper, H.H., Jacob, C.E., 1946. A generalized graphic method for evaluating formation

504   constants and summarizing well-field history. Transactions of American Geophysical Union.

505   27, 4, 526 – 534.

506   Dagan, G., 1967. Linearised solutions of free surface groundwater flow with uniform

507   recharge. Journal of Geophysical Research. 72, 4, 1183 – 1193.

508   Darling, W.G., Gooddy, D.C., Riches, J., Wallis, I., 2010. Using environmental tracers to

509   assess the extent of river–groundwater interaction in a quarried area of the English Chalk.

510   Applied Geochemistry. 25, 923 – 932.

511   Doherty, J., 2004. PEST: Model-independent parameter estimation user manual. Watermark

512   Numerical Computing

513   Gambolati, G., 1976. Transient free surface flow to a well: An analysis of theoretical

514   solutions. Water Resources Research. 12, 1, 27 – 39.

515   Hantush, M.S., Jacob, C.E., 1955. Non-Steady Radial Flow in an Infinite Leaky Aquifer.

516   Transactions of the American Geophysical Union. **36**, 95 – 100.

517   Harbaugh, A.W., 2005. MODFLOW 2005, The U.S. Geological Survey modular ground-

518   water model-the Ground-Water Flow Process: U.S. Geological Survey Techniques and

519   methods 6-16, variously p.

520   Kruseman, G.P., de Ridder, N.A., 1990. Analysis and evaluation of pumping test data. The

521   International Institute for Land Reclamation and Improvement. Publication 47.

522   Jackson, C.R., Hughes, A.G., Mansour, M.M., Spink, A.E.F., Bloomfield, J.P., Riches, J.,

523   Jones, M.A., 2003. Numerical modelling of a multiple-well pumping test using a locally

524   refined, object-oriented regional groundwater model. MODFLOW and More 2003:

525   Understanding through modelling, Conference Proceedings, Golden, CO, September 2003,

526   383 – 387.

527   Mansour, M.M., 2003. Flow to wells in unconfined aquifers using mesh refinement and

528   object-oriented technology. Ph.D. thesis. The University of Birmingham, UK.

529   Mansour, M.M., Spink, A.E.F., Riches, J., 2003. Numerical investigation of flow to pumped

530   wells in heterogeneous layered aquifers using radial flow models. MODFLOW and More

531   2003: Understanding through modelling, Conference Proceedings, Golden, CO, September

532   2003, 388 – 392.

533   McDonald, M.G., Harbaugh, A.W., 1988. A modular three-dimensional finite-difference

534   ground-water flow model. Technical report, U.S. Geol. Survey, Reston, VA.

535   Moench, A.F., 1993. Computation of type curves for flow to partially penetrating wells in

536   water-table aquifers. Ground Water, 31, 966 – 971.

537   Moench, A.F. 1994. Specific yield as determined by type-curve analysis of aquifer-test data.

538   Ground Water 6, 2, 37 – 46.

539   Moench, A.F. 1997. Flow to a well of finite diameter in a homogeneous, anisotropic water

540   table aquifer. Water Resources Research, 33, 6, 1397 – 1407.

541   Neuman, S.P., Witherspoon, P.A., 1971. Analysis of non-steady flow with a free surface

542   using the finite element method. Water Resources Research, 7, 3, 611 – 623.

543   Neuman, S.P., 1972. Theory of flow in unconfined aquifers considering delayed response of

544   the water table. Water Resources Research, 8, 4, 1031 – 1045.

545   Neuman, S.P., 1974. Effect of partial penetration on flow in unconfined aquifers considering

546   delayed gravity response. Water Resources Research, 10, 2, 303 – 312.

547   Neuman, S.P. 1979. Perspective on "delayed yield". Water Resources Research, 15, 899 –

548   908.

549   Reilley, T.E., Harbaugh, A.W., 1993. Simulation of cylindrical flow to a well using the U.S.

550   Geological Survey modular finite-difference groundwater flow model. Ground Water, 31, 3,

551   489 – 494.

552   Rushton, K.R., 2003. Groundwater Hydrology. Conceptual and computational model. John

553   Wiley and Sons Ltd, Chichester, UK.

554   Rushton, K.R., Redshaw, S.C., 1979. Seepage and groundwater flow. John Wiley and Sons,

555   Chichester, UK.

556   Streltsova, T.D. 1972. Unsteady radial flow in an unconfined aquifer. Water Resources

557   Research, 8, 4, 1059 – 1066.

558   Streltsova, T.D., 1973. Flow near a pumped well in an unconfined aquifer under nonsteady

559   conditions. Water Resources Research, 9, 1, 227 – 235.

560   Spink, A.E.F., Jackson, C.R., Hughes, A.G., Hulme, P.J., 2003. The benefits of object-

561   oriented modelling demonstrated through the development of a regional groundwater model.

562   MODFLOW and More 2003: Understanding through modelling, Conference Proceedings,

563   Golden, CO, September 2003, 336 – 340.

564   Spink, A.E.F., Mansour, M.M. 2003. Swanscombe Phase 2. Task 6: Preliminary Modelling.

565   Report prepared for the British Geological Survey. Wallingford, England.

566   Theis, C.V., 1935. The relation between the lowering of the piezometric surface and the rate

567   and duration of discharge of a well using groundwater storage. Transactions of the American

568   Geophysical Union, 16th annual meeting, 519 – 524.

569   Todsen, M., 1971. On the solution of transient free-surface problems in porous media by

570   finite-difference methods. Journal of Hydrology, 12, 177 – 210.

571

572

573

574

575

576

577

578

579

580

581

582

583

584

585

586

587

588

589

590

591   Figure 1: Regional setting of the Swanscombe area.

592   Figure 2: Conceptual model and numerical model setting at site C

593   Figure 3: Schematic representation of a multi-layered aquifer and the numerical

594   representation of quarries.

595

596   Figure 4: A typical time-drawdown curve obtained from pumping in unconfined
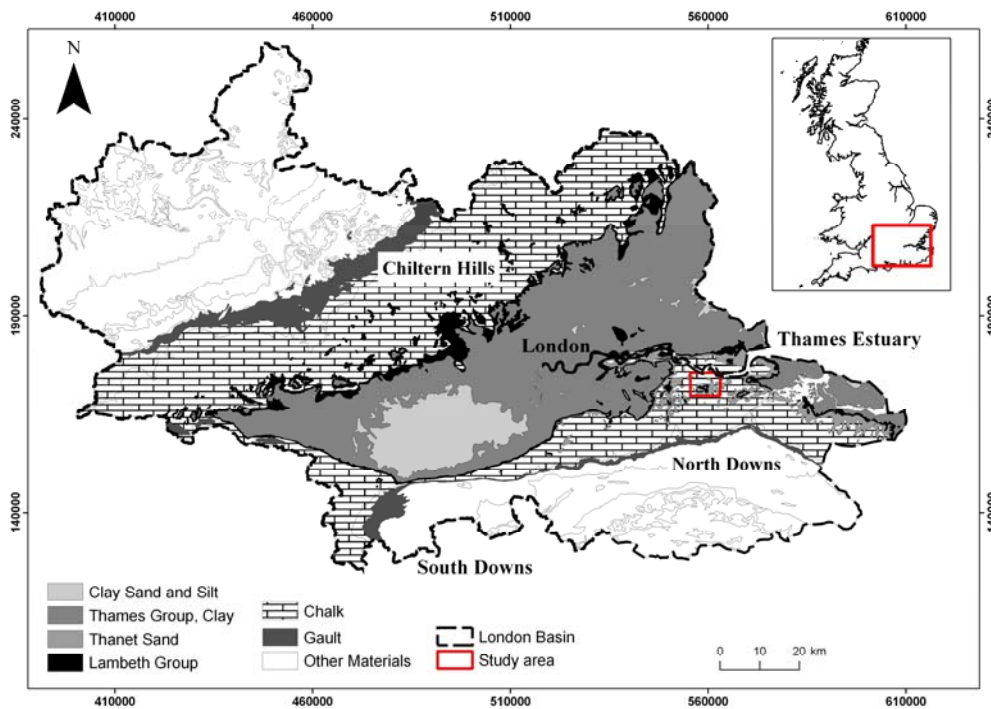
597   aquifers. (a): log-log scale. (b): log-arithmetic scale.

598   Figure 5: Field and numerical time-drawdown curves at Site C abstraction borehole

599   Figure 6: Field and numerical time-drawdown curves at Bean Farm and Eastern

600   Drudgeon Farm observation boreholes

601   Table 1: Optimised hydraulic parameter values and the 95% confidence limits.
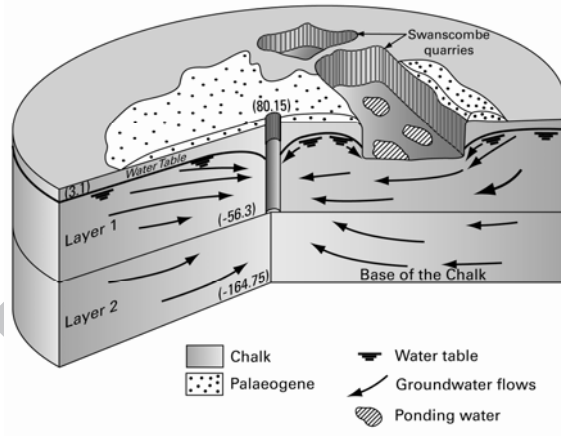
24

602

25

603   (a)

(b)

604

605

606

607

608

Partially penetrating
borehole with casing

Quarry

Water table
nodes

(H)

(V)   (V)

q_z

Upper Layer

Intermediate Layer

Lower Layer

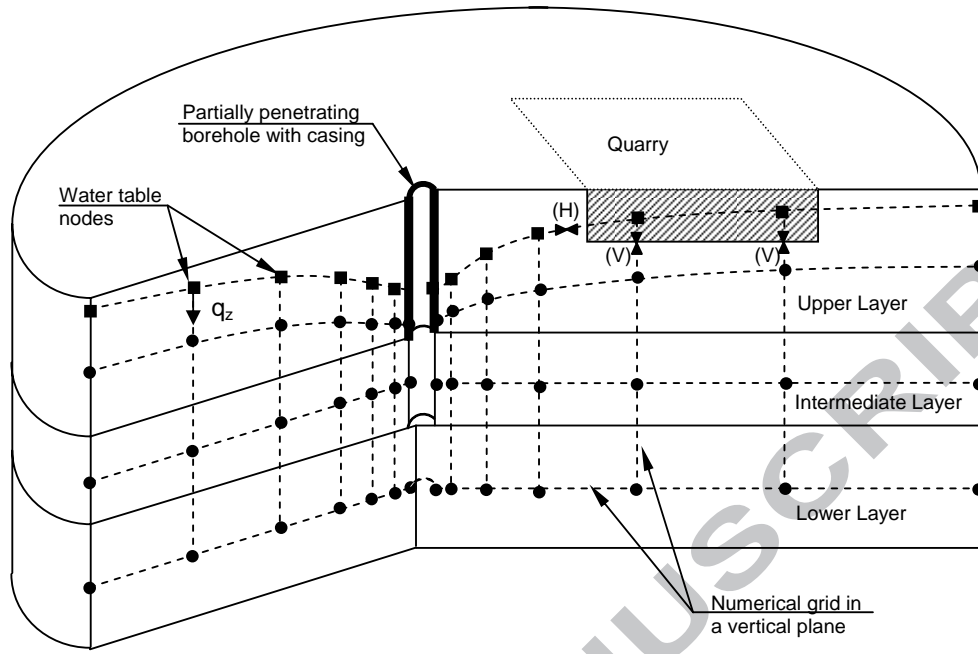Numerical grid in
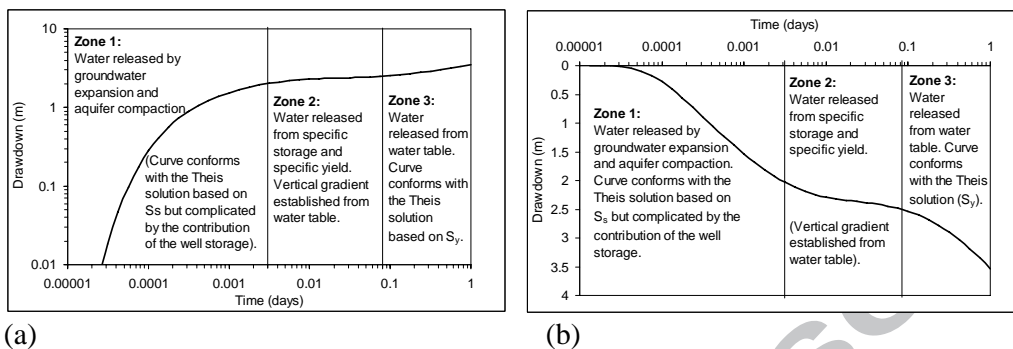a vertical plane

27
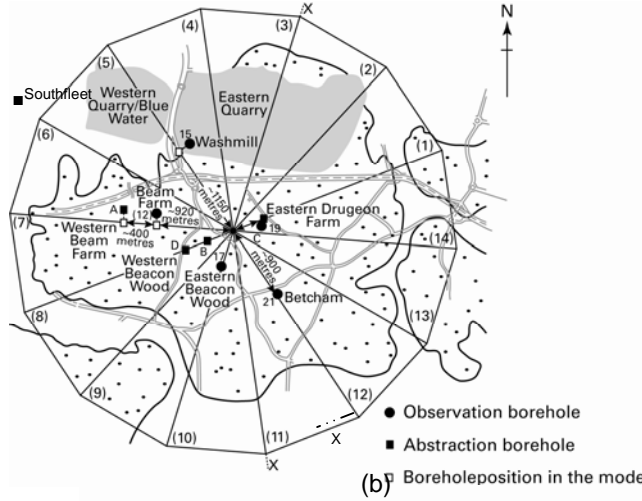
609

610

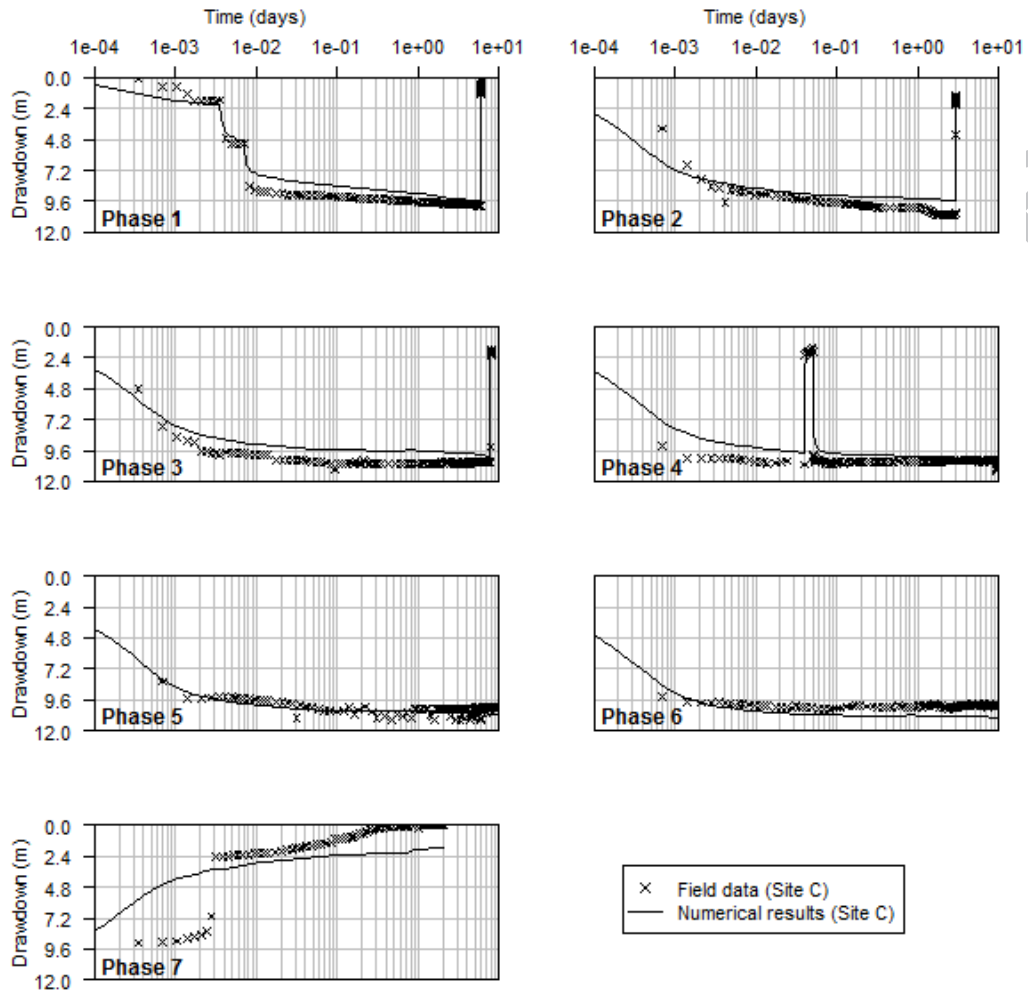611   (a)   (b)

612   Figure 5: A typical time-drawdown curve obtained from pumping in unconfined

613   aquifers. (a): log-log scale. (b): log-arithmetic scale.

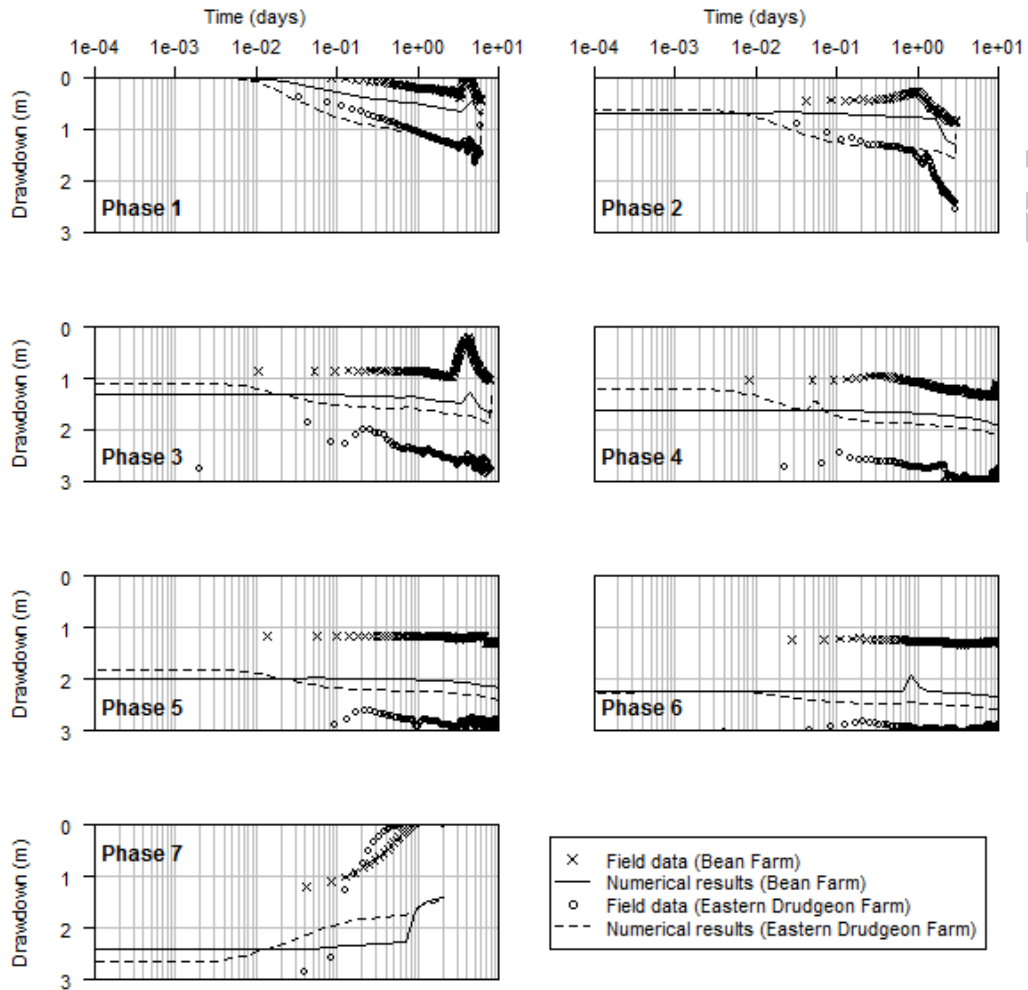614   finite-difference methods. Journal of Hydrology, 12, pp 177–210

615

616

617

618

619

620

621

622

623

624

625

626

627

628

629

Parameter	Estimated value	95% confidence limits	
		Lower limit	Upper limit
Horizontal hydraulic conductivity K_h (m day^{-1})	22.33	20.5	24
Vertical hydraulic conductivity K_v (m day^{-1})	0.086	0.065	0.107
Specific storage S_s (m^{-1})	1e-05	5.5e-06	14.5e-5
Specific yield S_y (dimensonless)	0.012	0.0087	0.015
Well loss factor (dimensionless)	0.09	0.072	0.109

630

631 **Research highlights**

632

633 A layered cylindrical grid model is used to analyse pumping test results
634 conducted in a quarried Chalk aquifer.

635 Quarries did not show significant impact the results unless nodes they occupy
636 are completely disconnected.

637 Numerical model is a powerful tool to test conceptual ideas.

638 Numerical model produces useful information regarding the hydraulic
639 characteristics of the aquifer.

640
641